Development of an all-fiber heterodyne lidar for range and velocity measurements

Fu Yang (杨 馥), Yan He (贺 岩), Jianhua Shang (尚建华), and Weibiao Chen (陈卫标)*

Shanghai Key Laboratory of All Solid-State Laser and Applied Techniques,
Shanghai Institute of Optics and Fine Mechanics, Chinese Academy of Sciences, Shanghai 201800, China
**E-mail:wbchen@mail.shcnc.ac.cn*

Received October 10, 2009

A 1550-nm all-fiber monostatic lidar system based on linear chirp amplitude modulation and heterodyne detection for the measurements of range and velocity is presented. The signal processing method is given, after which the relationship between the peak frequency values in the final signal spectrum, the target's range, and the line-of-sight velocity is obtained in the presence of the fiber end-face-reflected signal plaguing many monostatic lidar systems. The range of an electric fan as well as the line-of-sight fan speed of different levels is tested. This proposed system has a potential application for the space-borne landing system.

OCIS codes: 280.3640, 280.3340, 280.3400, 040.2840.
doi: 10.3788/COL20100807.0713.

The coherent lidar system plays a key role in planetary exploration and autonomous safe soft landing by providing precise range and velocity information. In fact, the space missions on the Moon and Mars launched by the NASA at locations with scientific values adopted this kind of system. Both the main oscillator and the local oscillator (LO) are frequency-modulated through a triangular frequency. By calculating the up-ramp and the down-ramp beat frequencies, the target distance and the relative line-of-sight velocity can be obtained[1]. In many frequency-modulated continuous wave (FMCW) laser radars[2], the transmitted waveform is often produced by linearly expanding or contracting the length of a laser resonator through a piezoelectric transducer (PZT). However, varying the length of a laser cavity is often undesirable since it can cause many problems, such as large phase noise and increased sensitivity to the environment[3]. In this letter, we propose a monostatic eye-safe 1550-nm laser lidar system combining the external linear positive chirp amplitude modulation through an electro-optical modulator (EOM) and the heterodyne detection[4,5]. All of the devices used in the system are off-the-shelf commercial products, guaranteeing stability while reducing research costs. Target range and velocity measurements are made using low peak laser power, long laser pulse, and a small telescope aperture.

The schematic of the system is shown in Fig. 1. The laser adopts a communication band of 1550 nm, which is safe for the eyes; it also adopts a single-mode continuous-wave (CW) fiber laser with a linewidth of 6 kHz[6]. The 50:50 beam coupler divides the laser into two equal parts. One part serves as the LO, while the other part serves as the main oscillator. The LO is frequency-shifted by 55 MHz through an acousto-optic modulator (AOM), whose drive signal is offered by a signal generator. The main oscillator is amplitude-modulated with a linear chirp signal by an EOM, whose drive signal is offered by a linear chirp signal generator. This signal generator can determine the bandwidth and pulse length of the linear chirp signal, which is the laser pulse length. The output of the EOM is entered into a circulator through port 1. An electric fan (San Jiao brand, Model No. Kyt25-802) was used as a target, to which the laser was transmitted through a telescope which used aspherical lens with an aperture of 3 cm. The return signal from the fan was collected by the same telescope and mixed with the LO in a 3-dB coupler. The optic devices of this system were connected by optical fibers, which, along with the monostatic setup, significantly simplified the optical adjustment. The mixed signal was then detected by a balanced photo detector, which had a common mode rejection ratio of 25 dB. The output of the photo detector was amplified and then sampled by a dual-channel 1-GHz 8-bit resolution analog-to-digital (A/D) converter. This signal is a broadband chirp signal modulated at 55 MHz. The other channel of the A/D converter sampled the chirp signals driving the EOM. The A/D converter and the chirp signal generator were triggered by the same electric circuit to ensure the time synchronization. All of the signal processing was carried out in a computer. The signal processing comprised the dechirp process, the in-phase and quadrature detection, filtering, and the combination of the in-phase and quadrature signals.

The chirp signal $m(t)$ can be expressed as

$$m(t) = \cos\left[2\pi\left(f_1 t + \frac{B}{2T}t^2 + \varphi_0\right)\right], \tag{1}$$

where f_1 and φ_0 are the chirp signal start frequency and the chirp signal initial phase, respectively, B is the bandwidth of the linear chirp signal, and T is the length of the laser pulse. The output of the circular port 3 signal in Fig. 1 can be formulated as

$$\begin{aligned} s(t) = {} & A_1[1 + m(t-\tau_1)]\cos(w_s t + \varphi_1) \\ & + A_2[1 + m(t-\tau_2)]\cos(w_s t + 2\pi f_{\mathrm{d}} t + \varphi_2), \end{aligned} \tag{2}$$

where A_1 and A_2 are the amplitudes of the fiber end-face-reflected signal and the target-reflected signal, τ_1 and τ_2

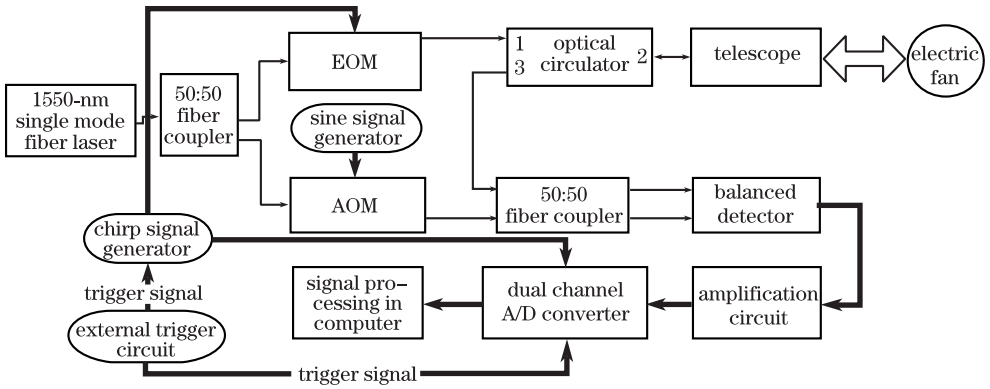

Fig. 1. Schematic of the coherent lidar system.

are the time delays caused by the fiber end face and the target, w_s and f_d are the main oscillator optical frequency and the Doppler frequency generated by the line-of-sight velocity of the target, φ_1 and φ_2 are the phases of the fiber end-face-reflected signal and the target-reflected signal, respectively.

The LO signal can be expressed as

$$L(t) = A_0 \cos(w_c t + \varphi_3), \tag{3}$$

where $A_0, w_c,$ and φ_3 are the amplitude, optical frequency, and phase of the LO, respectively.

The signal at the output of the balanced detector can be formulated as

$$\begin{aligned} s_0(t) = &\frac{1}{2} A_1 A_0 \cos(2\pi f_{\mathrm{AOM}} t + \varphi_4)[1 + m(t - \tau_1)] \\ &+ \frac{1}{2} A_2 A_0 \cos[2\pi(f_{\mathrm{AOM}} t + f_d t) + \varphi_5] \\ &\cdot [1 + m(t - \tau_2)], \end{aligned} \tag{4}$$

where f_{AOM} is the frequency-shifted by the AOM, $w_c = w_s + 2\pi f_{\mathrm{AOM}}$, φ_4 and φ_5 are the phase signals.

The dechirp process is normally carried out by mixing the detector output signal and the chirp drive signal together. It can be expressed as

$$\begin{aligned} s_1(t) = &\frac{1}{2} A_1 A_0 \cos(2\pi f_{\mathrm{AOM}} t + \varphi_4)[1 + m(t - \tau_1)] m(t) \\ &+ \frac{1}{2} A_2 A_0 \cos[2\pi(f_{\mathrm{AOM}} t + f_d t) + \varphi_5] \\ &\cdot [1 + m(t - \tau_2)] m(t). \end{aligned} \tag{5}$$

Using the band pass filter to extract the effective signal from Eq. (5), the filtered signal can be given as

$$\begin{aligned} s_2(t) = &\frac{1}{4} A_1 A_0 \cos(2\pi f_{\mathrm{AOM}} t + \varphi_4) \cos(2\pi f_1 t + \varphi_6) \\ &+ \frac{1}{4} A_2 A_0 \cos[2\pi(f_{\mathrm{AOM}} t + f_d t) + \varphi_5] \\ &\cdot \cos(2\pi f_2 t + \varphi_7), \end{aligned} \tag{6}$$

where $f_1 = \frac{B}{T}\tau_1$, $f_2 = \frac{B}{T}\tau_2$, and φ_6 and φ_7 are the phase signals.

The signal processing after the dechirp process comprises the in-phase (I) and quadrature (Q) detection; it is carried out by mixing $s_2(t)$ with the AOM drive signal. The I and Q signals are almost the same, except for the phase difference of 90°. The I and Q signals after the low-pass filtering with a bandwidth of f_{AOM} can be formulated as

$$\begin{aligned} I = &\frac{1}{8} A_1 A_0 \cos(\varphi_8) \cos(2\pi f_1 t + \varphi_6) \\ &+ \frac{1}{8} A_2 A_0 \cos(2\pi f_d t + \varphi_9) \cos(2\pi f_2 t + \varphi_7), \end{aligned} \tag{7}$$

$$\begin{aligned} Q = &\frac{1}{8} A_1 A_0 \sin(-\varphi_8) \cos(2\pi f_1 t + \varphi_6) \\ &- \frac{1}{8} A_2 A_0 \sin(2\pi f_d t + \varphi_9) \cos(2\pi f_2 t + \varphi_7). \end{aligned} \tag{8}$$

The fast Fourier transforms (FFTs) of the I and Q signals are expressed as

$$\begin{aligned} \mathrm{IFFT} = &\frac{1}{8} A_1 A_0 \cos(\varphi_8) \mathscr{F}[\cos(2\pi f_1 t + \varphi_6)] \\ &+ \frac{1}{8} A_2 A_0 \mathscr{F}[\cos(2\pi f_d t + \varphi_9) \\ &\cdot \cos(2\pi f_2 t + \varphi_7)], \end{aligned} \tag{9}$$

$$\begin{aligned} \mathrm{QFFT} = &\frac{1}{8} A_1 A_0 \sin(-\varphi_8) \mathscr{F}[\cos(2\pi f_1 t + \varphi_6)] \\ &- \frac{1}{8} A_2 A_0 \mathscr{F}[\sin(2\pi f_d t + \varphi_9) \\ &\cdot \cos(2\pi f_2 t + \varphi_7)]. \end{aligned} \tag{10}$$

The combination of I and Q signals is derived by summing up the square of the IFFT and QFFT. The combination signal is

$$\begin{aligned} \mathrm{SUM} = \mathrm{IFFT}^2 + \mathrm{QFFT}^2 = &\frac{1}{64} A_1^2 A_0^2 \mathscr{F}^2[\cos(2\pi f_1 t + \varphi_6)] + \frac{1}{64} A_2^2 A_0^2 \mathscr{F}^2[\cos(2\pi f_d t + \varphi_9) \cos(2\pi f_2 t + \varphi_7)] \\ &+ \frac{1}{64} A_2^2 A_0^2 \mathscr{F}^2[\sin(2\pi f_d t + \varphi_9) \cos(2\pi f_2 t + \varphi_7)] + \frac{1}{32} A_1 A_2 A_0^2 \cos(\varphi_8) \mathscr{F}[\cos(2\pi f_1 t + \varphi_6)] \\ &\mathscr{F}[\cos(2\pi f_d t + \varphi_9) \cos(2\pi f_2 t + \varphi_7)] + \frac{1}{32} A_1 A_2 A_0^2 \sin(\varphi_8) \mathscr{F}[\cos(2\pi f_1 t + \varphi_6)] \mathscr{F}[\sin(2\pi f_d t + \varphi_9) \cos(2\pi f_2 t + \varphi_7)]. \end{aligned} \tag{11}$$

There are five items in Eq. (11). As $\cos(2\pi f_1 t + \varphi_6)$, $\cos(2\pi f_\mathrm{d} t + \varphi_9)$, and $\cos(2\pi f_2 t + \varphi_7)$ have different peak values in the FFT, the product of $\mathscr{F}[\cos(2\pi f_1 t + \varphi_6)]$ and $\mathscr{F}[\cos(2\pi f_\mathrm{d} t + \varphi_9)\cos(2\pi f_2 t + \varphi_7)]$ can be ignored along with the fifth item. As a result, the last two items in Eq. (11) can also be ignored. Considering the three previous items, three peak values could be derived, namely, $F_1, F_2,$ and F_3, which are expressed as

$$F_1 = f_1, F_2 = |f_\mathrm{d} - f_2|, F_3 = f_\mathrm{d} + f_2. \tag{12}$$

Assuming $f_\mathrm{d} > f_2$, f_d and f_2 can be obtained by

$$f_\mathrm{d} = \frac{F_2 + F_3}{2}, f_2 = \frac{F_3 - F_2}{2}. \tag{13}$$

If $f_2 - f_1$ is the frequency in proportion to the true target distance, then the line-of-sight target velocity v and the target distance d_t can be calculated as

$$v = \frac{f_\mathrm{d}\lambda}{2} = \frac{(F_2 + F_3)\lambda}{4}, d_\mathrm{t} = \frac{cT(F_3 - F_2 - 2F_1)}{4B}. \tag{14}$$

The system parameters are shown in Table 1. The system distance resolution and velocity resolution can be expressed as

$$\Delta d_\mathrm{t} = \frac{c}{2B}, \Delta v = \frac{\lambda}{2T}, \tag{15}$$

where c is the speed of light. According to the values in Table 1, Δd_t and Δv are 3.75 m and 1.2 cm/s, respectively.

The laser transmits to the target, and the incident angle is almost vertical. Thus, the line-of-sight velocity is small. The electric fan has three speed levels, wherein level 1 is the slowest and level 3 is the fastest. We tested the system performance with varying fan speed levels while keeping the position of the fan constant. Using the above processing method, the final spectra with variable fan speed levels are shown in Fig. 2. Each spectrum is a single-shot measurement result, there are indeed three peaks in the final spectrum. According to the frequency values, the peaks are $F_1, F_2,$ and F_3 as shown in Eq. (12). The value of F_1 is constant in the three figures because F_1 corresponds to the fiber end-face-reflected signal. The values of F_2 and F_3 increase along with the rise in fan speed level. The space between F_2 and F_3 is almost the same regardless of the fan speed level since the space represents the target distance. Owing to the frequency resolution, the true peak frequency lies between neighboring quantization points. Taking the fiber end-face-reflected signal as an example, the true signal frequency lies between the second and the third quantization points, corresponding to the frequencies of 15.2625 and 30.525 kHz, respectively, the true peak frequency can be extracted[7].

After extracting the true peak frequency and by using Eq. (14), the respective line-of-sight target velocities and the true target distances corresponding to different levels are derived as follows: level 1, 1.008 m/s and 10.496 m; level 2, 1.433 m/s and 10.57 m; and level 3, 1.799 m/s and 10.453 m, respectively.

In conclusion, a 1550-nm all-fiber monostatic lidar system based on linear chirp amplitude modulation and heterodyne detection for the measurements of range and velocity is demonstrated. The derivation of the target range and the target line-of-sight velocity is given. The performance test shows that the system can detect the target distance and the target line-of-sight velocity accurately using low-transmitting power and small telescope aperture. Since the wavelength of the system is 1550 nm, the system is not only safe for the eyes, but also easy to be built from communication band commercial devices, ensuring robustness and stability of system. This system has great potential value in the future landing system, which requires both accurate relative range and velocity information.

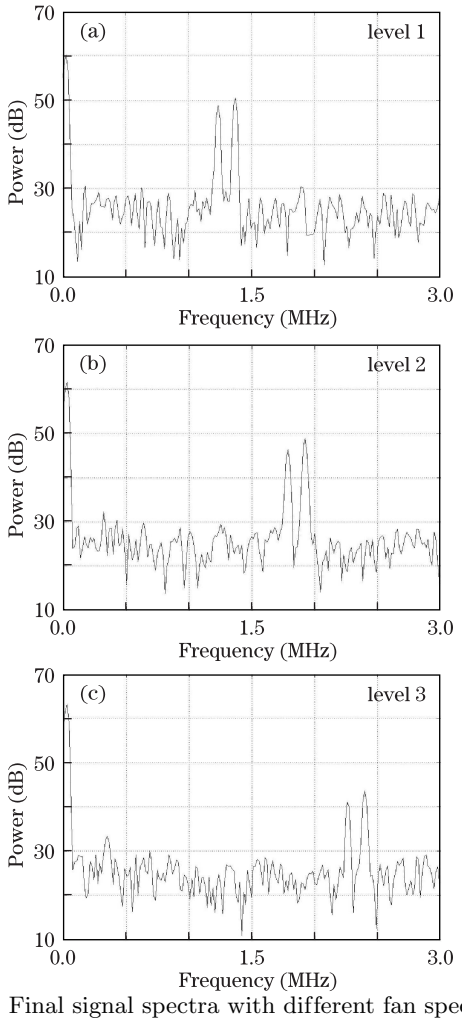

Fig. 2. Final signal spectra with different fan speed levels.

Table 1. System Parameters of the Linear Chirp Amplitude Modulation and Heterodyne Detection System

Transmitted Laser Peak Power	5 mW	LO Power	1.12 mW
Telescope Aperture	3 cm	Linear Chirp Bandwidth	40 MHz
Laser Pulse Length	65.52 μs	Target Distance	about 10 m
Target Type	Electric Fan	Transmitted Laser Mode	Focus at Target

References

1. D. Nordin, "Optical frequency modulated continuous wave (FMCW) range and velocity measurements" PhD. Dissertation (Luleå University of Technology, Scandinaria, 2004).
2. D. Pierrottet, F. Amzajerdian, and F. Peri, in *Mater. Res. Soc. Symp. Proc.* **883,** (2005).
3. C. Li, L. Duan, X. Yang, and Y. Chen, Acta Opt. Sin. (in Chinese) **29,** 2822 (2009).
4. C. T. Allen and S. K. Chong, "Development of a 1319-nm laser radar using fiber optics and RF pulse compression" Technical report (University of Kansas, 2002).
5. F. Yang, Y. He, and W. Chen, Acta Opt. Sin. (in Chinese) **28,** 573 (2008).
6. J. Shang, Y. He, D. Liu, H. Zang, and W. Chen, Chin. Opt. Lett. **7,** 732 (2009).
7. V. K. Jain, W. L. Collins, and D. C. Davis, IEEE Trans. Instrum. Measure **28,** 113 (1979).